




## Article

# A Study on the Ultimate Span of a Concrete-Filled Steel Tube Arch Bridge

Yuexing Wu <sup>1,2</sup>, Xiangchuan Wang <sup>3</sup>, Yonghui Fan <sup>2,\*</sup>, Jun Shi <sup>2</sup>, Chao Luo <sup>2</sup> and Xinzhong Wang <sup>1</sup>

<sup>1</sup> School of Civil Engineering, Hunan City University, Yiyang 413000, China; wuyuexing@hncu.edu.cn (Y.W.); 622210970020@mails.cqjtu.edu.cn (X.W.)

<sup>2</sup> State Key Laboratory of Mountain Bridge and Tunnel Engineering, Chongqing Jiaotong University, Chongqing 400074, China; 611200080015@mails.cqjtu.edu.cn (J.S.); luochao@mails.cqjtu.edu.cn (C.L.)

<sup>3</sup> Huasheng Testing Technology Co., Ltd., Chongqing 400039, China; 622220970001@mails.cqjtu.edu.cn

\* Correspondence: fyh1995@mails.cqjtu.edu.cn; Tel.: +86-17132308545

**Abstract:** In order to study the ultimate span of a concrete-filled steel tube (CFST) arch bridge, taking the structural strength, stiffness, and stability as the limiting conditions, the finite element analysis method is adopted to carry out research on the influence law of a single parameter of the pipe diameter, wall thickness, and cross-section height on the ultimate span of the arch axial shape. The result is used as a sample point to determine the ultimate span of the CFST arch bridge under multifactor coupling based on the response surface method. The finite element method is used to check the strength, stiffness, stability, number of segments and maximum lifting weight, steel content rate, and steel pipe concrete constraint effect coefficient of the CFST arch bridge under the ultimate span diameter. The results show that, when analyzed using a single parameter, the ultimate span diameter of the CFST arch bridge increases with the increase in the steel pipe diameter and the cross-section height, and then decreases. Moreover, it increases with the increase in the wall thickness of the steel pipe, and the CFST arch bridge reaches the ultimate span with the increase in the steel pipe wall thickness. When the pipe diameter is 1.38 m, the CFST arch bridge reaches the ultimate span; according to a multi-parameter coupling analysis, when the pipe diameter is 1.49 m, wall thickness is 37 mm, and cross-section height is 17 m, the CFST arch bridge reaches the ultimate span of 821 m, which meets all of the limiting conditions, and, at this point, the arch axial coefficient is 1.2. The results of the finite element calculation show that the structural strength, prior to the stiffness, stability, and other limitations, just reaches the critical value of the limiting conditions.

**Keywords:** concrete-filled steel tube arch bridge; ultimate span; strain energy minimization method; finite element analysis; response surface method



**Citation:** Wu, Y.; Wang, X.; Fan, Y.; Shi, J.; Luo, C.; Wang, X. A Study on the Ultimate Span of a Concrete-Filled Steel Tube Arch Bridge. *Buildings* **2024**, *14*, 896. <https://doi.org/10.3390/buildings14040896>

Academic Editor: Fabrizio Gara

Received: 21 February 2024

Revised: 19 March 2024

Accepted: 23 March 2024

Published: 26 March 2024



**Copyright:** © 2024 by the authors. Licensee MDPI, Basel, Switzerland. This article is an open access article distributed under the terms and conditions of the Creative Commons Attribution (CC BY) license (<https://creativecommons.org/licenses/by/4.0/>).

## 1. Introduction

With the increasing improvement of arch bridge design theory, the application of high-strength materials, and the advancement of cable-stayed buckling construction technology, large-span CFST arch bridges are becoming increasingly more prevalent [1]. At present, the largest CFST arch bridge in the world is the Pingnan Three Bridge in Guangxi, with a main span of 575 m. Zheng [2] pointed out that China has the ability to design and build 700 m class CFST arch bridges. However, no matter how developed the theory and construction technology of this type of bridge is, it is difficult to increase the span diameter endlessly. The limit to which the span diameter of CFST arch bridges can reach is no longer included in the program comparison, which is a matter of concern for bridge designers [3]. The study of the ultimate span diameter of CFST arch bridges is of great scientific significance and engineering application value for the deep understanding of the mechanical behavior of the steel pipe and the concrete in the pipe, when they work in coordination, and for the improvement of the design methods and specifications of this type of bridge.

The current domestic and international research on the ultimate span diameter of arch bridges can be mainly divided into three categories.

The first category focuses on improving the span diameter of arch bridges by optimizing the structural form [4–6]. For example, Xie et al. [7] proposed a new bridge structural system known as the medium-bearing cable arch bridge; here, the main span and side spans of suspension bridges are set up in the arch rib and the main cables are anchored to the arch foot of the side arches, and the structural mechanical performance is improved by adjusting the yaw-to-span ratio. A study was carried out with a 700 m span as an example, and the results showed that this structural form improved the strength-bearing capacity and stability-bearing capacity by about 25% and 70%, respectively, compared with a continuous arch bridge under the same conditions, which lays a solid foundation for a breakthrough in the improvement of the arch bridge span. To address the problem that the large self-weight of arch bridges restricts the development of the spanning diameter, Huang et al. [8] put forward a new type of arch structure consisting of top concrete, bottom concrete, and steel web rods (Steel-Reinforced Concrete, SRC). The calculation results showed that the self-weight of the new type of arch rib was reduced by about 31% compared with the original bridge, and nearly one-third of the construction time of the arch rib pouring concrete could be saved, which has certain feasibility in design and construction technology. This kind of research improves the span diameter by optimizing the structural form but pays less attention to the theoretical span limit of this structural form of arch bridge.

The second type of research focuses on improving the span diameter of arch bridges by using high-strength materials [9,10]. Zhang et al. [11] used theoretical derivation to analytically determine the ultimate span diameter of arch bridges and studied the ultimate span diameter of the bridges when R200 activated fly ash concrete and Q690 high-strength steel were used. The researchers found that the theoretical ultimate span diameter of concrete arch bridges using R200 activated powder concrete can reach up to 2000 m, while the main span of steel arch bridges using Q690 high-strength steel can be greater than 2500 m. Shao et al. [12] carried out the conceptual design of a 1000 m class arch bridge based on steel–ultra-high-performance fiber-reinforced concrete (UHPFRC). The results of a finite element analysis showed that the design solution meets the structural stability, strength, and stiffness requirements of the code. This type of research increases the span diameter of the arch bridge by improving the strength of the material but neglects the sharp increase in the construction difficulty after this increase in span diameter [13].

The third category of research primarily investigates the mechanical performance of concrete-filled steel tube (CFST) composite members from the component level. For instance, Wei et al. [14] conducted dynamic performance tests on CFST composite columns, indicating that a higher axial compression ratio leads to earlier yield initiation and more severe final failure of the specimens. Additionally, Wang et al. [15] performed axial compression bearing capacity tests on 18 short steel tube concrete columns, analyzing the impact of basalt fiber length on their mechanical properties. Compared to conventional short steel tube concrete columns, the addition of basalt fibers significantly enhanced the axial compression-bearing capacity and ductility coefficient of the columns, with average increases of approximately 8.1% and 31.6%, respectively. Zhang et al. [16] conducted dynamic performance tests and numerical simulation analyses on eight Recycled Aggregate Concrete-Filled Circular Steel Tube (RACFCST) specimens, noting that the load-bearing capacity of these specimens decreased with an increase in the axial compression ratio and with a reduction in the beam–column linear stiffness ratio and yield bending moment ratio. Additionally, Zhang et al. [17] explored the dynamic performance of S-RACFCST specimens and proposed a displacement-based seismic design method for S-RACFCST frames, verifying that this method meets the requirements for “temporary use”, “normal use”, and “collapse prevention”. Such studies mainly focus on the performance optimization and pattern analysis of specimens, failing to deeply explore the potential and efficacy of CFST composite members within the overall structure, particularly regarding their role and contribution to the design of large-span arch bridges. Although CFST composite members exhibit excellent

performance in enhancing local mechanical properties, research on their application in overall structural design, construction technology, and long-term performance remains relatively scarce.

In summary, current research on the ultimate span of arch bridges primarily exhibits three issues: a focus on structural optimization while neglecting theoretical limits, an emphasis on the application of high-strength materials without considering construction difficulties, and a concentration on the mechanical performance optimization of specimens without a systematic study of structural aspects from design and construction to long-term performance. In view of these shortcomings, this study selects several key factors affecting the span diameter of large-span steel-tube concrete arch bridges, taking into account the feasibility of the structural design, construction programs, and other constraints to examine the influence of these factors on the ultimate span of the bridges. This approach is combined with the response surface method to comprehensively consider the coupling effect between a number of factors on the acquisition of the ultimate span of steel-tube concrete arch bridges, and to provide a reference for the promotion of the arch bridges for the development of a greater span diameter.

## 2. Study of Reasonable Parameters for the Limit Span

### 2.1. Parameter Selection

In conducting research on the ultimate span of CFST arch bridges, the rationality of parameter selection is crucial to the reliability of the research results. Considering several key factors, such as structural geometry, material mechanical properties, section-bearing capacity, and structural stability, four types of parameters, namely, arch axial shape, material strength, section height, and height-to-span ratio, are selected for this study [18–20].

#### 2.1.1. Rationalization of the Arch Axis

The selection of the arch axis is the basis of arch bridge design. Under the action of external load, the main arch rib only produces axial pressure. Without bending moment and shear force, the arch axis and the pressure line completely coincide; such an arch axis is known as a reasonable arch axis [21], and its determination must follow the principle of the line shape being reasonable, aesthetically appealing, and convenient to construct.

According to statistics, large-span steel pipe concrete is mostly used in hollow-belly arch bridges [22]. The constant load set of this type of structure is distributed discontinuously along the arch ribs, and the suspension chain line is a curve that matches its pressure line. The authors of [23] investigated the proportion of suspension chain lines, parabolic lines, and spline curves as arch axes in CFST arch bridges in China, and pointed out that 66.67% of CFST arch bridges used suspension chain lines as arch axes. Currently, the Poseidon Yangtze River Bridge with a main span of 530 m, the Hejiang Yangtze River Highway Bridge with a main span of 507 m, and the Pingnan Third Bridge with a main span of 560 m [24] all use suspended chain lines as arch axes.

In summary, the suspension chain line is formulated as the arch axis line shape for the limit span study in this paper. It can be seen through the equation of the hanging chain line that the selection of the arch axis coefficient  $m$  of the hanging chain line is closely related to the load set on the arch, and the load sets of arch bridges under different spans are different, so the research process of the ultimate span should be carried out in accordance with the existing optimization method of the arch axis coefficient under the optimal arch axis coefficient.

#### 2.1.2. Material Parameters

The steel pipe concrete structure is a combination of structures consisting of a steel pipe filled with concrete, and this creates a concrete hoop effect so that the steel pipe is in a three-direction compression state. This combined structure has the advantages of high strength, light weight, good ductility, fatigue resistance, impact resistance, and other good mechanical properties.

According to statistics [25], with the increase in the arch bridge span and the need for structural strength, the proportion of Q345 steel used in CFST arch bridges increases year by year, and C60 or even C70 concrete is also gradually being applied in large-span CFST arch bridges. In the 507 m Hejiang Yangtze River Bridge, and in the world's largest-spanning steel arch bridge, the Pingnan Bridge, the upper and lower chords are made of Q345 steel pipe and C70 concrete. Some builders of large-span arch bridges have begun to use Q420 steel [26]; the concrete in the tube is self-compacting compensatory concrete, and the strength grade is mostly C60~C80 [27]. Combined with the development trend of the material and the current application prospects, this paper adopts the combination of Q420 steel and C80 concrete for the subsequent ultimate span study.

### 2.1.3. Cross-Sectional Construction Parameters

The arch rib section is one of the most important aspects of arch bridge design. According to statistics relating to the arch rib section forms of 327 CFST arch bridges [28], the four-limbed truss section is used most often in large-span CFST arch bridges, so this research adopts the four-limbed truss section for the study of ultimate span.

For the truss section, the steel pipe concrete diameter, wall thickness, cross-section truss height, and variable cross-section mode are the key parameters of design, and the reasonableness of their values directly affects the structural stress performance. The values of some CFST arch bridge section parameters in China are summarized in Table 1.

**Table 1.** Values of cross-section parameters of some steel pipe arches in China.

Serial Number	Bridges	Span (m)	Pipe Diameter (m)	Wall Thickness (mm)	Section Height Ratio Foot/Top of Arch
1	Guangxi Pingnan Third Bridge	560	1.4	34	2.0 (17 m/8.5 m)
2	Sichuan Hejiang Bridge	530	1.3	30	2.0 (16 m/8.0 m)
3	Sichuan Hejiang Yangtze River Highway Bridge	507	1.32	32	2.0 (14 m/7.0 m)
4	Wushan Yangtze River Bridge	492	1.22	25	2.0 (14 m/7.0 m)
5	Guizhou Dazaijing Bridge	450	1.36	35	1.8 (14 m/8 m)
6	Yunnan Mengxin Highway Liangshuigou Bridge	430	1.2	35	2.0 (13 m/6.5 m)
7	Hunan Xiangtan Liancheng Bridge	388	0.85	24	1.8 (9 m/5 m)
8	Hunan Yiyang Maocaojie Bridge	368	1	28	2.0 (8 m/4 m)
9	Guizhou Zongxi River Bridge	360	1.2	35	1.8 (11 m/6 m)

From referencing the aforementioned information and taking into account the manufacturing capabilities of steel structure factories, the range for the pipe diameter in the limit span analysis process of this study is 1260 mm~1500 mm, the wall-thickness range is 32 mm~48 mm, the truss-height range is 13 m~24 m, and the ratio of the cross-section height of the foot of the arch to the top of the arch takes a value of 2.

### 2.1.4. Height-to-Span Ratio

The height-to-span ratio refers to the ratio of the span to the height of the main arch rib, the value of which affects the structural stress performance and the degree of coordination between the structure and the external environment.

For CFST arch bridges, the arch rib height-to-span ratio should be suitable in the range of 1/6~1/4, considering appearance, landscape, construction difficulty, etc. [29]. According to the statistical analysis of the height-to-span ratio of the constructed truss CFST arch bridges in China [30], most of the height-to-span ratios are concentrated at 1/5 or 1/4, accounting for as much as 66%, and taking a larger height-to-span ratio value within a reasonable range is conducive to the overall performance of the arch ribs; thus, a height-to-span ratio of 1/4 is proposed in this study to carry out the subsequent ultimate spanning diameter analysis.

## 2.2. Limit Indicators for Limit Span Analysis

In order to overcome the problem that the existing research cannot take into account the inadequacy of structural design, material strength, construction methods, and other factors, and the fact that the selected material strength, structural stiffness, stability, number of main arch segments, maximum lifting weight of the segments, steel content of the steel pipe concrete, steel pipe concrete constraint effect coefficients, and steel pipe diameter and thickness ratios are research process limitations in combination with the current specification requirements, the limitations of the indicators take the following values:

In terms of material strength, Q420 steel and C80 concrete are selected as the materials for the upper and lower chords of the steel pipe concrete, and the design values of the axial compressive strength and axial tensile strength of the C80 concrete are taken as 34.6 MPa and 2.14 MPa, respectively. The design values of the strength of the Q420 steel are taken as 320 MPa (wall thickness of 16–40 mm) or 305 MPa (wall thickness of 40–63 mm).

In terms of structural rigidity, the maximum vertical deflection of the main arch under lane loading should not be greater than  $L/1000$  ( $L$  is the span diameter).

In terms of stability, the elastic overall stability coefficient of the main arch should not be less than 4.0 in the construction and operation use stage, and the stability coefficient of the local components should not be less than the elastic overall stability coefficient of the main arch.

Regarding the number of main arch sections and the maximum lifting weight of the sections, with reference to the equipment transfer capacity of the existing bridge construction process, the proposed number of single-rib section divisions shall not exceed 32 sections, and the maximum lifting weight of the sections shall not exceed 200 tons.

The steel content of the steel pipe concrete (the ratio of the steel pipe area to the concrete area in the cross-section) ranges from 0.04 to 0.20, the steel pipe concrete constraint effect coefficient (the ratio of the product of the area of the steel pipe and the design value of the steel strength to the product of the area of the concrete and the design value of the concrete strength in the cross-section) should not be less than 0.6, and the ratio of the steel pipe diameter to thickness should range from 40 to 90.

## 2.3. Parametric Coupling Analysis Methods

Finite element software is used to determine the influence of multiple parameters on the ultimate span of CFST arch bridges, which has a huge computational workload and can only obtain the analytical value rather than the functional relationship equation. Meanwhile, in the process of studying the ultimate span diameter, parameters such as material, construction parameters, arch axis coefficient, and height-to-span ratio are in a mutually coupled relationship, for which the response surface method can be used to analyze and solve. The response surface method [31] is a statistical method of experimental design and optimization used to study the effects of multiple factors on one or more response variables and to determine the optimal conditions, which has the advantages of being able to analyze multiple variables, reduce the number of tests, and be visualized [32]. In this paper, the response surface model is used to replace the complex finite element calculation model, and the combination of the design of experiments and the response surface method establishes a mathematical model of the limit span diameter, which can considerably improve the efficiency of the ultimate span determination process. The specific steps are as follows: First, an analysis of the impact of various parameters on the ultimate span of CFST (concrete-filled steel tube) arch bridges is conducted based on the finite element model. Subsequently, using the analysis results as sample data, a response surface function for the ultimate span of CFST arch bridges is obtained by fitting the sample data. This function is then subjected to an F-test and  $R^2$  test. Following this, a mathematical optimization model for the ultimate span of CFST arch bridges is established, yielding the ultimate span under various constraints. Finally, the optimization results are verified through the finite element model.

### 3. Reasonable Arch Axis Analysis

#### 3.1. Arch Axis Line Analysis

The arch axis coefficient  $m$ , as the linear characteristic value of the suspension chain line [33], depends on the arch axis coefficient to a large extent. In order to ensure that the deviation between the suspension chain line and the load pressure line is small, it is necessary to adopt a reasonable arch axis coefficient optimization method to solve this coefficient, and, with the change in the cross-section parameters, spanning diameter, and other parameters, the value of the reasonable arch axis coefficient is not certain; thus, the study of the ultimate spanning diameter needs to be based on the optimal arch axis coefficient.

#### 3.2. Optimization Method for Reasonable Arch Axis Coefficients

The arch rib bending strain energy minimization method [34] is a commonly used arch axis coefficient optimization method for large-span arch bridges which controls the value of bending moments in each section of the arch rib by controlling the deviation of the arch axis from the load pressure line. The principle is as follows:

In the elastic range of the structure, the elastic deformation energy  $U$  of an elastomer due to deformation under external load is numerically equal to the work carried out  $W$  by the external load on the corresponding displacement:

$$U = W \quad (1)$$

where the elastic strain energy  $U$  can be expressed as

$$U = \int_l \frac{M(x)^2}{2EI} dx + \int_l \frac{Q(x)^2}{2GA} dx + \int_l \frac{N(x)^2}{2EA} dx \quad (2)$$

where  $\int_l \frac{M(x)^2}{2EI} dx$  denotes the bending energy caused by the bending moment  $M$ ,  $\int_l \frac{Q(x)^2}{2GA} dx$  denotes the shear energy caused by the shear force  $Q$ , and  $\int_l \frac{N(x)^2}{2EA} dx$  denotes the axial deformation energy caused by the axial force  $N$ ;  $E$  and  $G$  denote the modulus of elasticity and shear modulus of the material, respectively; and  $I$  and  $A$  denote the moment of inertia and the area of the cross-section, respectively.

The magnitude of the strain energy can reflect the stress state of the structure. For compression structures such as arch bridges, the ideal main arch rib force form should only bear the axial force and not the bending moment and shear force. Therefore, for the design of the arch bridge structure, the bending deformation energy and shear deformation energy of the main arch rib need to be as small as possible so that the structure remains mostly unaffected by the bending moment and shear force. The shear deformation energy is generally only about 5% of the bending deformation energy [35], which may not be considered. Therefore, in the selection of arch-axis alignment for arch bridges, the bending strain energy minimum method can be considered for the optimization of arch-axis alignment:

$$U = \int_l \frac{M(x)^2}{2EI} dx \quad (3)$$

For discrete rod system units, Equation (3) can be modified to

$$U = \sum_{i=1}^m \frac{l_i}{4E_i I_i} (M_{Li}^2 + M_{Ri}^2) \quad (4)$$

where  $m$  is the total number of structural units;  $L_i$ ,  $E_i$ , and  $I_i$  are the element length, modulus of elasticity, and section bending moment of inertia of element  $i$ ; and  $M_{Li}$  and  $M_{Ri}$  are the left- and right-end bending moments of element  $i$ .

#### 4. Analysis of the Effect of Different Parameters on the Ultimate Spanning Diameter

##### 4.1. Methods for Analyzing the Effect of Different Parameters on the Ultimate Span Diameter

In this paper, the ultimate span study of the CFST arch bridge is based on the suspension chain line. As the arch axis line shape and the suspension chain line shape are controlled by the arch axis coefficient  $m$  as a single variable, the value of which is closely related to the set of loads on the arch, the ultimate span study process needs to determine the optimal arch axis coefficient under each parameter, such as the diameter of the steel pipe and the wall thickness.

According to the parameter value range formulated in Section 2.1, a steel pipe concrete arch bridge is taken as the engineering basis, and finite element analysis and calculations are carried out according to the established step length. In the process of calculation, firstly, according to the control variables to be studied, a set of initial state parameters for the structure is selected, the corresponding finite element model is established, and the optimal arch axis coefficient corresponding to the set of parameters is searched by minimizing the eccentricity distance of the cross-section; then, strength, stiffness, and stability analyses are carried out. If all of these factors are in the proposed limiting conditions, then the span diameter is increased and analyzed again according to the above steps until any one of the strength, stiffness, and stability analysis results exceeds the limiting value. In this case, the calculation is stopped, and the current span is recognized as the limit span under the group of parameters. Subsequently, according to the above steps, the values of the ultimate span of the sample points increase according to the proposed step length until each group of variables is obtained, and the trend of the changes in the ultimate span under different variables is also obtained. A flowchart of the study on the ultimate span of the CFST arch bridge is shown in Figure 1.

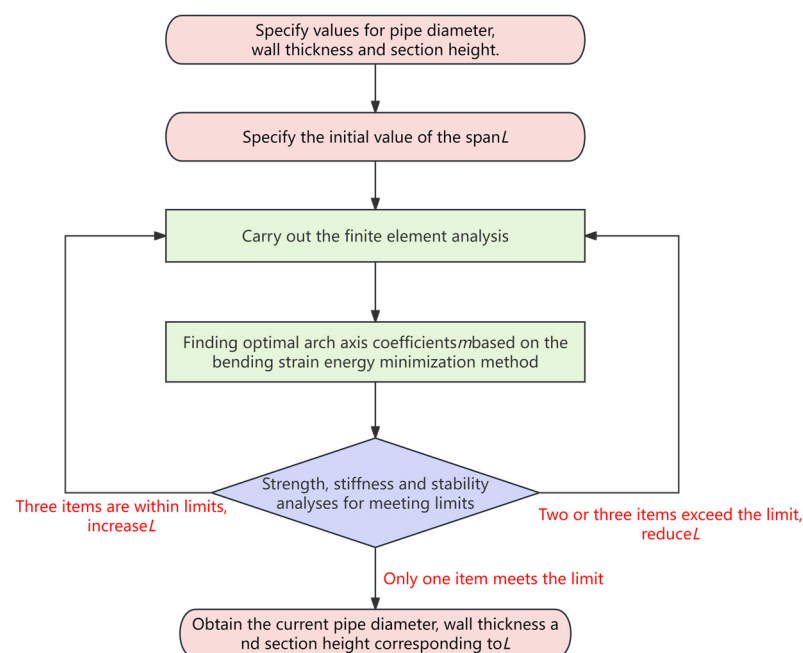


**Figure 1.** Flowchart for the study of the trend of the influence of single-parameter variation on the ultimate span diameter.

##### 4.2. Finite Element Calculation Models

###### 4.2.1. Project Overview

The Hejiang Yangtze River Highway Bridge is located in Hejiang, Luzhou City, Sichuan Province. The main bridge structure is the swallow-type steel pipe concrete tie arch bridge, and the main arch ribs use steel pipe concrete truss sections. The span arrangement is (80.5 + 507 + 80.5) m with a total length of 668 m, and the bridge is the world's largest-

spanning arch bridge. The net height-to-span ratio of the main span is 1/4, the arch axis coefficient is 1.5, and the spacing between the arch ribs on both sides is 25.3 m. The radial height of the arch top cross-section is 7.0 m, and that of the arch foot cross-section is 14 m. The layout of the bridge is shown in Figure 2.

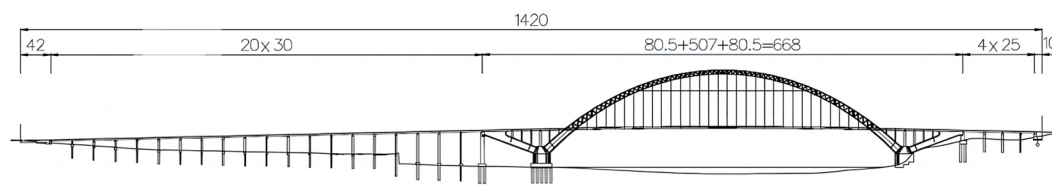


**Figure 2.** Bridge layout (unit: meter).

#### 4.2.2. Finite Element Model

Combined with the structural characteristics of the Hejiang Yangtze River Highway Bridge, this study adopts Midas Civil V2.1 finite element analysis software to establish a three-dimensional rod system calculation model. The finite element model of the Hejiang Yangtze River Highway Bridge is shown in Figure 3.



**Figure 3.** Finite element model of Hejiang Yangtze River Highway Bridge.

A total of 9607 nodes and 23,014 elements are established in the finite element simulation of the Hejiang Yangtze River Highway Bridge, and different element types are adopted according to different structural stress states and considerations. Among them, the suspension rods are simulated by the tensile truss elements, the stiffened plate at the foot of the arch and the steel bridge panels are simulated by the shell elements, and the rest are simulated by the beam elements. The steel pipe is made of Q345 steel: the modulus of elasticity is taken as  $2.06 \times 10^5$  MPa and the Poisson's ratio is taken as 0.3. The concrete in the pipe is C70 concrete: the modulus of elasticity is taken as  $3.7 \times 10^4$  MPa and the Poisson's ratio is taken as 0.2. When analyzing the structure, the displacements and rotations at the base of the arch seat and both abutments are constrained. Elastic connections are used between the main arch rib and the columns on the arch, and between the columns and the main beams, with geometric nonlinearities taken into account in the calculations, which only consider the structural deadweight loads.

#### 4.2.3. Validation of Finite Element Models

In order to verify the correctness of the finite element model, the theoretical elevation and the measured elevation of the arch rib were compared after the main arch ring was merged and loosened, and the results are shown in Figure 4.



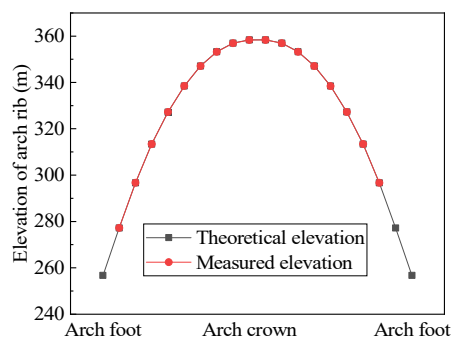


**Figure 4.** Comparison between theoretical and measured elevation of arch rib.

In Figure 4, the measured and theoretical elevation curves of the arch rib basically coincide with each other, and the maximum relative error is 34 mm, which occurs at the top of the arch, with a maximum relative error of 0.03%, verifying the correctness of the finite element model.

#### 4.3. Analysis of the Effect of Pipe Diameter on the Ultimate Span

In order to study the change trend of the pipe diameter and ultimate span of the CFST arch bridge, the wall thickness of the steel pipe, height-to-span ratio, cross-section parameter, and material type were formulated as constants, and the change trend of the ultimate span of the CFST arch bridge under the corresponding parameter was studied by changing the pipe diameter. The optimal arch axis coefficients of the suspension chain line under the seven groups of different pipe diameter values for the main arch static analysis calculations, in order to meet the strength, stiffness, and stability of the corresponding parameter under the ultimate span value, are shown in Table 2, and an illustration of the pipe diameter and the trend of the ultimate span diameter is shown in Figure 5.

**Table 2.** Ultimate spans of steel pipe concrete arch bridges corresponding to different pipe diameters.

Pipe Diameter (m)	Wall Thickness (mm)	Height of Arch Foot Section (m)	Height of Vault Section (m)	Height-to-Span Ratio	Optimum Arch Axis Coefficient	Ultimate Span (m)
1.26	32	14.24	7.12	1/4	1.35	737
1.30					1.35	768
1.34					1.30	776
1.38					1.30	784
1.42					1.30	780
1.46					1.35	758
1.50					1.35	751

According to Figure 5, it can be concluded that, with the increase in the cross-section pipe diameter, the limit span value under the corresponding parameter shows a trend of increasing and then decreasing. At the peak apex of the curve, i.e., when the diameter of the steel-concrete pipe is taken as 1.38 m, the stress of the steel pipe of the lower chord under the optimal arch axial shape of the hanging chain line reaches the limit value, and the span cannot be further increased. On the left side of the peak point of the curve, the compressive and flexural stiffness of the concrete section of the steel pipe increases with the increase in the diameter of the steel pipe, which leads to the growth of the ultimate span; however, on the right side of the peak point of the curve, in the case of the constant wall thickness of the steel pipe, the proportion of the steel pipe that bears the constant load stress increases with the increase in the diameter of the steel pipe, and the proportion of the rate of increase is greater than that of the compressive stiffness of the concrete section of the steel pipe. Therefore, the stress of the steel pipe increases gradually and exceeds the

allowable strength of the material, which results in a gradual decrease in the ultimate span under the corresponding parameter.

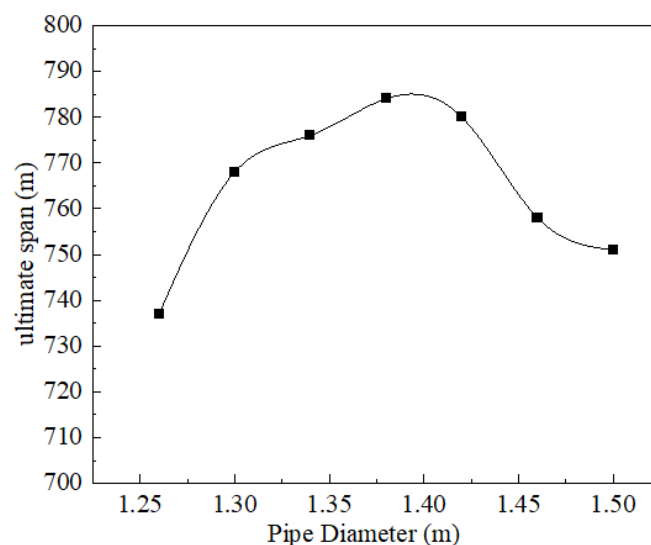


**Figure 5.** Effect on ultimate span under pipe diameter change.

#### 4.4. Analysis of the Effect of Pipe Wall Thickness on Ultimate Span

In order to study the change trend of the wall thickness of the steel pipe in the main arch section and the ultimate span of the CFST arch bridge, the diameter of the steel pipe, concrete pipe, truss height, height-to-span ratio, cross-section parameters, and material type were formulated as constants, and the change in the ultimate span of the CFST arch bridge was studied by changing the wall thickness of the steel pipe concrete under the corresponding parameters. Based on the optimal arch axis coefficient of the hanging chain line, the main arch static analysis was calculated for five groups of different wall thickness values, and the ultimate span values were obtained under the corresponding parameters to satisfy the strength, stiffness, and stability. The values are shown in Table 3, and the trend of the wall thickness and ultimate span is shown in Figure 6.

**Table 3.** Ultimate span corresponding to different tube wall thicknesses.

Pipe Diameter (m)	Wall Thickness (mm)	Height of Arch Foot Section (m)	Height of Vault Section (m)	Height-to-Span Ratio	Optimum Arch Axis Coefficient	Ultimate Span (m)
1.5	0.032	20	10	1/4	1.40	710
	0.036				1.30	780
	0.040				1.25	850
	0.044				1.20	900
	0.048				1.20	960

As can be seen from Table 3 and Figure 6, the ultimate span of the CFST arch bridge increases approximately linearly with the increase in the wall thickness of the steel pipe, which is due to the fact that, with the increase in the steel content in the cross-section, the stresses in the steel pipe and in the concrete are gradually reduced, which allows the value of the ultimate span of the structure to be further increased. The steel content is 9.11% at a wall thickness of 32 mm, and increases to 10.33%, 11.58%, 12.85%, and 14.14% according to the proposed increase in step length, corresponding to an increase in the ultimate span of 8.94%, 16.03%, 21.06%, and 25.62%, which shows that an increase in the wall thickness increases the value of the ultimate span of the corresponding parameter.

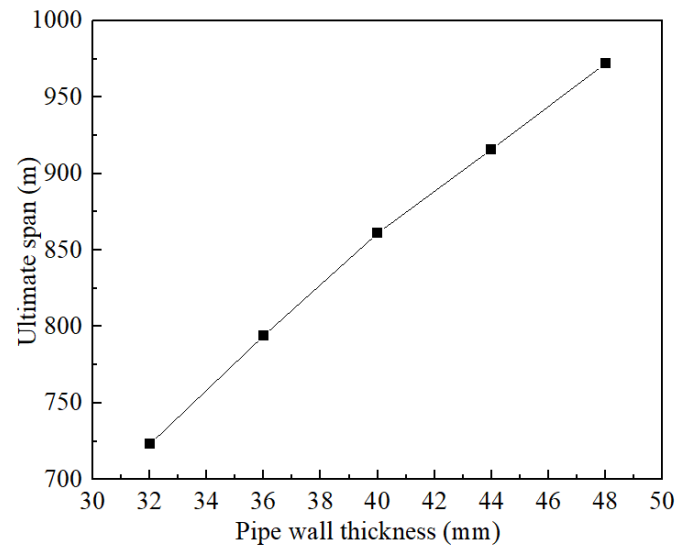


**Figure 6.** Ultimate spans of CFST arch bridges with different steel tube wall thicknesses.

#### 4.5. Analysis of the Effect of Section Height on Ultimate Span Diameter

In order to study the trends for the main arch cross-section truss height and the ultimate span of the CFST arch bridge, the steel pipe concrete diameter, wall thickness, height-to-span ratio, cross-section parameter, and material type were set as constants, and the trend of the ultimate span of the CFST arch bridge under the corresponding parameter was investigated by changing the cross-section height. Based on the optimal arch axis coefficient of the hanging chain line, 11 groups of different truss heights were calculated for the static analysis of the main arch rib. The values of the ultimate span under the corresponding parameters of strength, stiffness, and stability are shown in Table 4, and the trend of the truss height and the ultimate span is plotted in Figure 7.

**Table 4.** Table of ultimate span parameters for main arch with different section heights.

Pipe Diameter (m)	Wall Thickness (mm)	Height of Arch Foot Section (m)	Height of Vault Section (m)	Height-to-Span Ratio	Optimum Arch Axis Coefficient	Ultimate Span (m)
1.5	40	14	7.0	1/4	1.30	800
		15	7.5		1.25	850
		16	8.0		1.20	885
		17	8.5		1.25	875
		18	9.0		1.25	865
		19	9.5		1.25	858
		20	10.0		1.25	850
		21	10.5		1.30	836
		22	11.0		1.30	820
		23	11.5		1.30	805
		24	12.0		1.30	810

According to Table 4 and Figure 7, with the increase in the cross-section truss height, the limit span value under the corresponding parameter shows a trend of increasing and then decreasing. At the peak of the curve, i.e., when the height of the foot of the arch truss is taken as 16 m, the stress of the steel pipe of the lower chord under the optimal arch axis shape of the suspension chain line reaches the limit value, and the span cannot be further increased. The bending stiffness of the section of the arch foot increases with the increase in the section height, but the stability coefficients of each order of the main arch ring first decrease slowly and then increase rapidly with the increase in the section height. This is due to the fact that the stability of the main arch ring is affected by both the

section stiffness and the span diameter at the same time, and the favorable influence of the former is greater than the unfavorable influence of the latter when the section height is in the range of 14–16 m. The opposite is true when the section height is more than 16 m, which ultimately results in the increase and then the decrease in the ultimate span diameter of the CFST arch bridge with the increase in the section height.

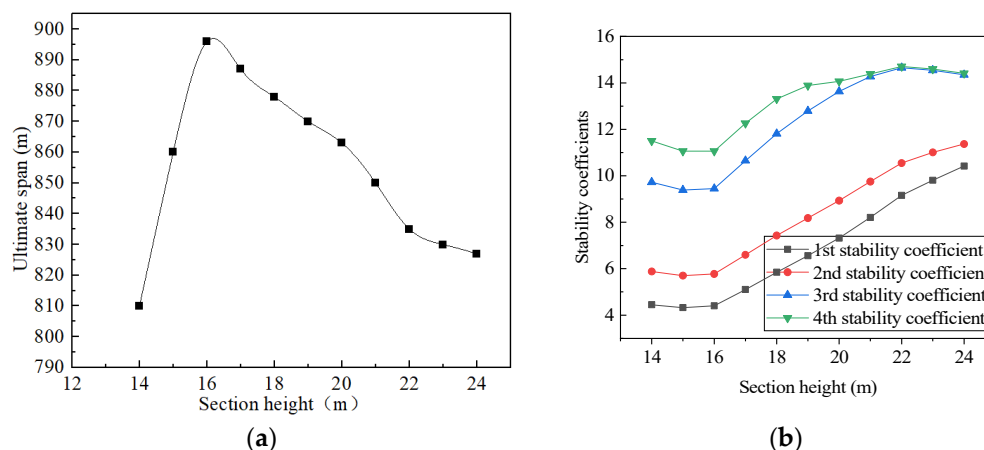


**Figure 7.** Ultimate span and stability coefficients of main arch ribs at different section heights. (a) Ultimate span at different section heights of the main arch rib; (b) stability coefficients of the first four orders of the main arch rib under different cross-section heights.

## 5. Ultimate Spanning Analysis Based on Response Surface Methodology

In the previous section, the effect of single-parameter changes, such as pipe diameter, wall thickness, and section truss height, on the ultimate span of a CFST arch bridge was investigated, and the analysis process only considered the three constraints of structural strength, stiffness, and stability. In this section, the number of section divisions and the maximum lifting weight of the sections, steel content rate, constraint effect coefficient, and diameter/thickness ratio are increased in order to study the ultimate span of a CFST arch bridge with four additional constraints.

However, through the change of a single variable and according to the proposed step size exhaustive calculation, the workload is huge, the iterative process is complicated, and only the numerical solutions can be obtained rather than the functional equation. This section describes the use of the response surface method for the ultimate spanning diameter; the solution process uses the results from Section 4 as the sample point data, uses the response surface model instead of the complex finite element computation model, and establishes the ultimate spanning diameter mathematical model, which can significantly improve the efficiency of the ultimate spanning diameter determination process.

### 5.1. Multiple Nonlinear Regression Analysis Based on Response Surface Methodology

The response surface method (RSM) analyzes the response surface and contour lines to seek the optimal parameters. This approach uses multiple quadratic regression equations to fit the response value and the factors of the functional relationship between the optimization of statistical methods. The basic idea is to test the system of the target response value as a function of a number of experimental factors, and such a functional relationship occurs through the derivation of the means of the optimization of the experimental design of the optimal parameters, i.e., the deterministic sample points are tested in order to achieve the goal of fitting a response surface to approximate the distribution of response values.

### 5.2. Mathematical Modeling of Response Surfaces for Extreme Spans

#### 5.2.1. Identification of Sample Points and Sample Data

The study variables of steel pipe concrete diameter, wall thickness, and cross-section joist height are denoted as  $x_1$ ,  $x_2$ , and  $x_3$ , with units of m, mm, and m, respectively, and

the study range of the variables is formulated as  $x_1 \in (1.26, 150)$ ,  $x_2 \in (32, 48)$ , and  $x_3 \in (14, 24)$ . The study range of the variables is defined as follows.

The finite element response value  $y$  is the limiting span under the corresponding parameter, i.e., the sample point data, which are obtained using finite element analysis software calculations. Considering the interval distribution of the sample points and the fact that the appropriate increase in the number of sample points can improve the fitting accuracy, and based on the center combination test design method, a total of 41 groups of sample point data were extracted. The sample points and finite element response values are shown in Table 5.

**Table 5.** Sample points and corresponding ultimate spans of steel tube concrete arch bridges.

Finite Element Response Value $y$	Random Variable			Finite Element Response Value $y$	Random Variable		
Ultimate Span (m)	$x_1$	$x_2$	$x_3$	Ultimate Span (m)	$x_1$	$x_2$	$x_3$
737	1.26	32	16.76	760	1.26	32	16.00
768	1.30	32	16.84	735	1.26	32	19.00
776	1.34	32	16.92	700	1.26	32	24.00
784	1.38	32	17.00	790	1.34	32	16.00
780	1.42	32	17.08	755	1.34	32	19.00
758	1.46	32	17.16	730	1.34	32	24.00
751	1.50	32	17.24	790	1.42	32	16.00
800	1.50	40	14.00	760	1.42	32	19.00
850	1.50	40	15.00	735	1.42	32	24.00
885	1.50	40	16.00	795	1.26	36	16.00
875	1.50	40	17.00	830	1.26	36	19.00
865	1.50	40	18.00	812	1.26	36	24.00
858	1.50	40	19.00	825	1.34	36	16.00
850	1.50	40	20.00	833	1.34	36	19.00
836	1.50	40	21.00	810	1.34	36	24.00
820	1.50	40	22.00	835	1.42	36	16.00
805	1.50	40	23.00	850	1.42	36	19.00
810	1.50	40	24.00	825	1.42	36	24.00
710	1.50	32	20.00	850	1.50	40	20.00
780	1.50	36	20.00				

### 5.2.2. Limit Span Response Surface Fitting and Accuracy Tests

In this paper, the ultimate span study considers the parameter correlation and chooses the second-order polynomials containing cross terms as the basic equations of the response surface model:

$$y = a + \sum_{i=1}^n b_i x_i + \sum_{i=1}^n \sum_{j=1}^n c_{ij} x_i x_j \quad (5)$$

where  $a$  is a constant term,  $x_i$ ,  $x_i x_j$  is the basis function of the response surface model,  $n$  is the number of random variables, and  $a$ ,  $b_i$ ,  $c_{ij}$  are the coefficients of the basis function.

According to the 41 groups of sample points and sample data formulated in Section 5.2.1, the model of the response surface containing only significant terms is fitted based on stepwise regression to obtain the response surface function of the ultimate span of the steel pipe concrete arch bridge. The coefficients of the response surface function and the results of the accuracy test are shown in Tables 6 and 7 below.

**Table 6.** Response surface modeling function coefficients.

Basis Functions	Constant	$x_1^2$	$x_1$	$x_2$	$x_3$
Extreme Span Response Surface Modeling	−3182.68	−1887.04	4973.20	−0.43	41.10
Basis Function	$x_2^2$	$x_3^2$	$x_1 x_2$	$x_1 x_3$	$x_2 x_3$
Limit Span Response Surface Model	−0.23	−0.89	15.59	−17.68	0.41

**Table 7.** Sample points and corresponding ultimate spans of steel tube concrete arch bridges.

Response Surface Modeling	F-Test	$R_{adj}^2/\%$
Extreme span response surface	124.42	95.40

The F-test mentioned in Table 7 is a statistical method used to determine that at least one of the coefficients in the model is significantly non-zero. In response to the surface methodology, it is primarily used to test the significance of the entire regression model. If the  $p$ -value of the F-test is less than a certain threshold, the entire model is considered significant, i.e., at least one of the predictor variables in the model has a significant effect on the response variable. The coefficient of determination  $R^2$  is a statistic that measures the goodness of fit of a model, with a value between 0 and 1.  $R^2$  describes the degree to which the independent variable in the model explains the variation in the response variable. An  $R^2$  value close to 1 means that the model explains most of the variation in the response variable, and in response surface methodology, higher  $R^2$  values usually indicate a better model fit to the data.

In practice, the F-test and  $R^2$  are often used in conjunction to assess the statistical significance and goodness-of-fit of a model. The F-test tells us whether the model is significant overall, while the  $R^2$  provides a quantitative measure of the model's ability to account for variation. Considering both statistics together can be used to assess the validity and fitness of a model.

The maximum value of the critical F value is 3.41 at a significance level of  $\alpha = 0.05$ . From Table 7, it can be seen that the F value of the extreme spanning response surface model is 124.42, which is much larger than the critical F value, indicating that the response surface model is significant. From Table 7, it can be seen that the  $R_{adj}^2$  value is 95.4%, which indicates that 95.4% of the total deviation of the extreme spanning response surface model under the corresponding parameter is caused by the change in the random variable, i.e., the total response is not explained by the resulting response surface model, and, at most, 4.6% of the deviation cannot be explained by the resulting response surface model. The fitting accuracy of the response surface model is high, and the obtained response surface model is reliable and can be used for the subsequent solving of the limiting spanning values that satisfy each constraint.

### 5.3. 1:10 Optimization of the Response Surface Model for Extreme Spanning Solutions

#### 5.3.1. Mathematical Model for Limit Span Optimization

The steel pipe concrete diameter, wall thickness, and section truss height are selected as design variables, which are labeled as  $x_1$ ,  $x_2$ , and  $x_3$ , and the ultimate span diameter is selected as the objective function. Under the restriction indexes formulated in Section 2.2, the maximum value of the ultimate span of the steel pipe concrete arch bridge can be achieved, and then the ultimate span optimization problem can be expressed as follows:

$$\left\{ \begin{array}{l} \max F \\ 1.26 \leq x_1 \leq 1.5 \\ 32 \leq x_2 \leq 48 \\ 14 \leq x_3 \leq 24 \\ 0.04 \leq \frac{A_s}{A_c} = \frac{x_1^2}{(x_1 - 2x_2)^2} - 1 \leq 0.2 \\ \zeta = \frac{420}{50.2} \times \left( \frac{x_1^2}{(x_1 - 2x_2)^2} \right) \geq 0.6 \\ x_1/x_2 \geq 0.04 \end{array} \right. \quad (6)$$

where  $A_s/A_c$  denotes the cross-section steel content of the steel pipe concrete member;  $A_s$  and  $A_c$  denote the total area of steel reinforcement and the total area of concrete in the cross-section, respectively; and  $\zeta$  denotes the coefficient of the confinement effect of the steel pipe concrete.

In order to more intuitively analyze the relationship between the study variables and the objective function as the ultimate spanning diameter, the response surface model for the ultimate spanning diameter was analyzed graphically and intuitively using the computational analysis software MATLAB R2018a.

The trend of the ultimate spanning response surface with respect to the study variables  $x_2$  and  $x_3$  when the study variable  $x_1 = 1.4$  is shown in Figure 8, the trend of the ultimate spanning response surface with respect to the study variables  $x_1$  and  $x_3$  when the study variable  $x_2 = 36$  is shown in Figure 9, and the trend of the ultimate spanning response surface with respect to the study variables  $x_1$  and  $x_2$  when the study variable  $x_3 = 20$  is shown in Figure 10.

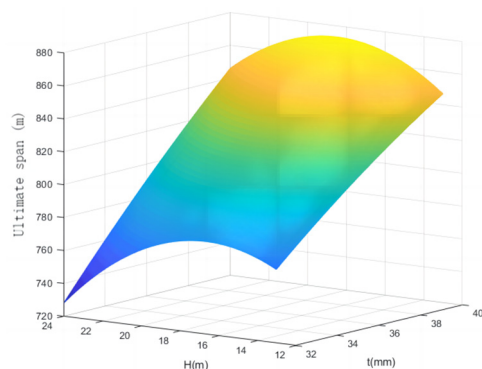


**Figure 8.** Limit span response surface  $x_1 = 1.40$ .

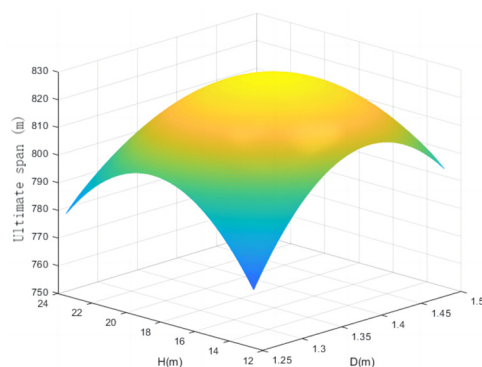


**Figure 9.** Limit span response surface  $x_2 = 36$ .

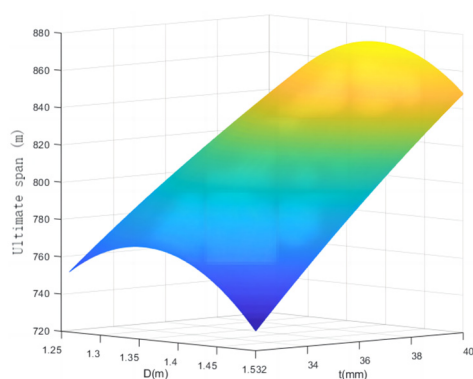


**Figure 10.** Limit span response surface  $x_3 = 20$ .

The above Figures 8–10 showing the variation surface of the limit span with the study variables clearly reflect the response values and the direction of finding the maximum limit span at different values of the variables. The change in color from blue to yellow in Figures 8–10 represents the increase in ultimate span from small to large.

According to the ultimate span response surface model and the optimization mathematical model, the optimization toolbox of MATLAB and the multivariate nonlinear optimization function were used to optimize and solve the problem and ultimately reached the optimum at  $x_1 = 1.49$ ,  $x_2 = 37$ , and  $x_3 = 17$ , corresponding to the value of an ultimate span of 821 m and an optimal arch axis coefficient of 1.2.

This ultimate span exceeds the span of the current largest CFST arch bridge in the world, the Guangxi Pingnan Third Bridge, which has a main span of 575 m; this represents a span increase of 246 m (42.78%), indicating that CFST arch bridges still have significant potential for development in large-span bridges.

It should be additionally noted that, when an i5-11300H four-core CPU with 16G RAM is used to carry out the optimization calculations, the optimization time is no more than 1 min, which is much less than the time required using finite element analysis, verifying the high level of efficiency of the response surface method for determining the ultimate span of CFST arch bridges.

### 5.3.2. Finite Element Verification of Optimization Results

According to the above findings, in order to verify the correctness of the optimization results based on the response surface model, the maximum ultimate span and the corresponding structural parameters of the optimization solution were calculated using finite element analysis. The maximum ultimate span finite element model is shown in Figure 11.

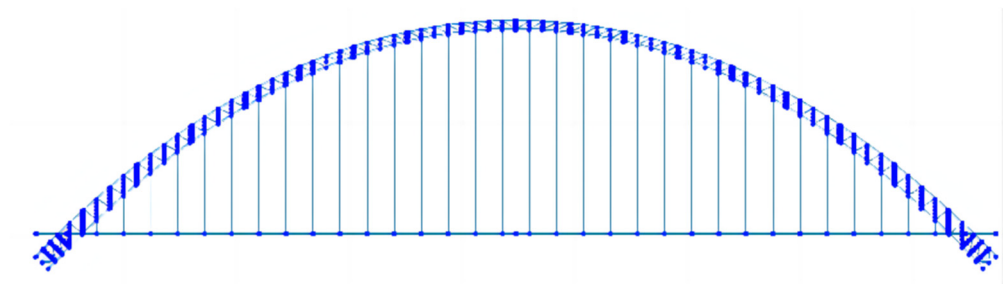


**Figure 11.** Finite element modeling of maximum ultimate span of CFST arch bridge.

The results of the strength calculations of the steel pipe and the concrete in the pipe under the combination of the basic effects of the ultimate load-carrying capacity state are shown in Figure 12.

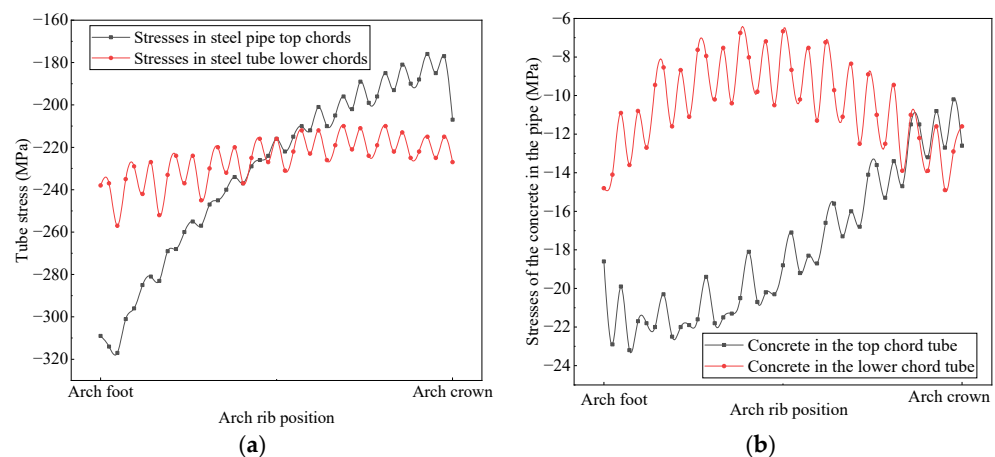


**Figure 12.** Main arch rib stress simulation results. (a) Stress distribution along the span of steel pipe stringers; (b) stress distribution along the span of the concrete in the pipe.

As can be seen from Figure 12, the maximum stresses of the steel pipe and concrete in the pipe appear at the foot of the arch, and the stresses of the steel pipe and concrete in



the pipe in the upper chord are more uniformly distributed along the span, with a large increase in the middle of the span. The stresses of the steel pipe and concrete in the pipe in the lower chord gradually decrease along the distribution of the span, and the steel pipe and the concrete in the pipe are in a state of compression. The maximum stress values under load are as follows:

$$\begin{cases} (\sigma_s)_{\max} = |-317.81| \text{MPa} \leq 320 \text{ MPa} \\ (\sigma_c)_{\max} = |-23.80| \text{MPa} \leq 34.6 \text{ MPa} \end{cases} \quad (7)$$

According to the maximum stress value, it can be seen that the concrete stress reserve in the pipe is large, and the maximum stress value of the steel pipe is approaching the strength limit value. At this time, the limit span continues to increase with the strength of the steel pipe.

The maximum vertical deflection of the main arch of the CFST arch bridge under lane loads (excluding impact forces) is shown in Figure 13.

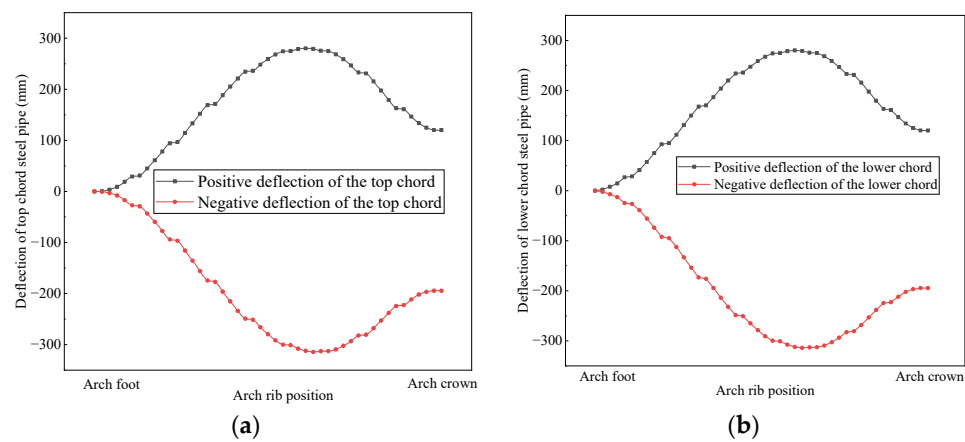


**Figure 13.** Distribution of steel pipe deflection along the span diameter. (a) Distribution of deflection of top chord steel pipe along span diameter; (b) distribution of deflection of lower chord steel pipe along span diameter.

From Figure 13, it can be seen that the deflection extremes of the upper and lower chord bars under lane loading (not counting the impact force) both appeared at  $1/4L$ , and the maximum vertical deflection value was as follows:

$$W_{\max} = 593.21 \text{ mm} \leq \frac{L}{1000} = 829.00 \text{ mm} \quad (8)$$

An elastic buckling stability analysis was carried out for the overall and local stability of the steel pipe concrete main arch only. The buckling analysis was carried out using the Midas civil space finite element model with the moving load equivalent concentrated force as a variable load and other loads as a constant load. The results of the first four orders of instability modal calculations are shown in Figure 14.

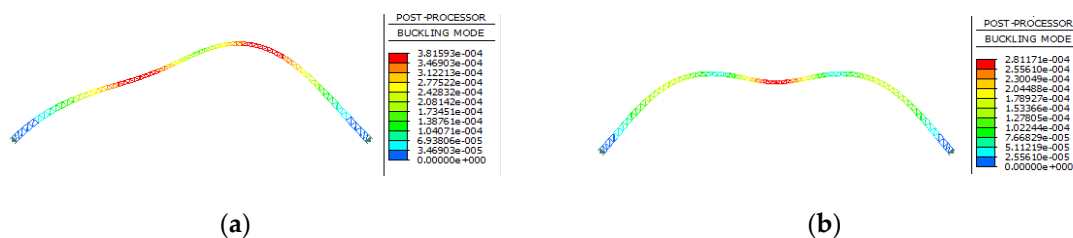


**Figure 14.** Cont.

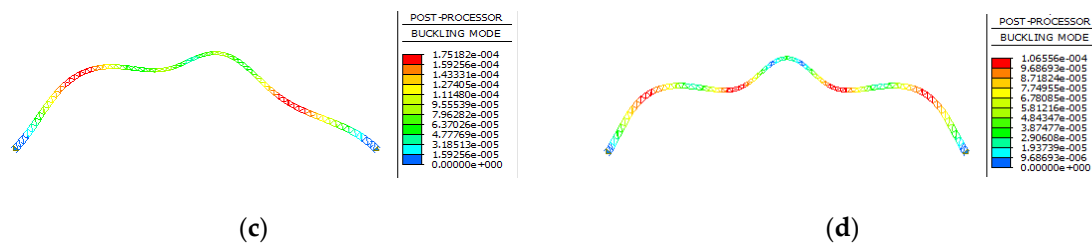


**Figure 14.** Modal diagram of the first four orders of instability of the main arch rib. (a) The 1st instability modal diagram of the main arch rib; (b) 2nd instability modal diagram of the main arch rib; (c) 3rd instability modal diagram of the main arch rib; (d) 4th instability modal diagram of the main arch rib.

The first four orders of instability forms and elastic buckling stability coefficients during the operational phase of the completed bridge are shown in Table 8.

**Table 8.** Sample points and corresponding ultimate spans of CFST arch bridges.

Order	Destabilized Mode	Elastic Flexural Stability Coefficient
1st destabilization	In-plane antisymmetric instability	6.33
2nd destabilization	In-plane symmetric instability	9.07
3rd destabilization	In-plane antisymmetric instability	14.49
4th destabilization	In-plane symmetric instability	17.30

From the instability modal diagrams presented in Figure 14 and the elastic buckling stability coefficients shown in Table 8, it can be seen that the elastic buckling stability coefficients of all orders are greater than the allowable values.

The CFST arch bridge steel structure arch rib (excluding the transverse brace) weighs a total of 12,512 t. Single rib lifting can be divided into 32 segments, with the maximum lifting weight segment control of 200 t, to meet the proposed restrictions.

Steel pipe concrete contains steel at a rate  $\alpha_s$  of:

$$0.04 \leq \alpha_s = \frac{A_s}{A_c} = \frac{x_1^2}{(x_1 - 2x_2)^2} - 1 = 0.108 \leq 0.2 \quad (9)$$

The steel content meets the limits drawn up in accordance with the specifications.

The steel pipe concrete constraint effect coefficient  $\zeta$  is:

$$\zeta = \frac{420}{50.2} \times \left( \frac{x_1^2}{(x_1 - 2x_2)^2} \right) = 0.89 \geq 0.6 \quad (10)$$

The constraint effect coefficients satisfy the constraints drawn up in accordance with the specification.

## 6. Conclusions

In order to study the ultimate span of a CFST arch bridge, taking the structural strength, stiffness, and stability as the limiting conditions, the finite element analysis method was adopted to examine the trend of the influence of the change in a single parameter of the pipe diameter, wall thickness, and truss height on the ultimate span on the basis of the optimal analysis of the arch axial shape. The response surface method was introduced into the optimization of the ultimate span to solve the problem, and then the value of the ultimate span of the CFST arch bridge was obtained. The main conclusions are as follows:

(1) The diameter of the steel pipe concrete and the corresponding parameters of the ultimate span diameter showed a trend of increasing and then decreasing. When the

diameter of the steel pipe concrete was taken as 1.38 m, the stress of the lower chord steel pipe reached the limiting value under the optimal arch axial shape of the suspension chain line; the wall thickness of the steel pipe concrete and the corresponding parameters of the ultimate span diameter showed a trend of continuous increase; and the truss height of the main arch cross-section and the corresponding parameters of the ultimate span diameter showed a trend of increasing and then decreasing.

(2) An optimization method based on the response surface method was proposed to solve the ultimate spanning diameter, and the response surface model of the ultimate spanning diameter was established by taking the pipe diameter, wall thickness, and truss height as the research variables, and the response surface function of the ultimate spanning diameter with high reliability was obtained. By establishing the ultimate spanning diameter optimization mathematical model and adopting the multivariate nonlinear optimization function for the optimization and solution, a maximum value of the ultimate spanning diameter of 821 m was reached when the pipe diameter was 1.49 m, the wall thickness  $t$  was 37 mm, and the truss height was 17 m, satisfying all the constraints. The optimal arch axis coefficient was 1.2.

(3) The verification analysis was carried out using finite element software, and the results showed that the structural strength just reached the limit value, and the remaining variables, such as the stiffness, stability, and the maximum lifting weight of the section, were all within the limit values.

Environmental factors, as important factors affecting the construction quality of large-span CFST arch bridges, restrict the span development of these bridges to a certain extent. Mountain canyon winds, ambient temperatures, construction schemes, etc., tend to directly affect the structural stability, deformation, and stress during the construction of arch bridges, and carrying out a study on the ultimate spans of CFST arch bridges that considers environmental factors and the actual construction scheme used will be the next step in our research.

**Author Contributions:** Conceptualization, Y.W. and X.W. (Xiangchuan Wang); methodology, Y.W. and Y.F.; software, Y.W.; validation, C.L., J.S. and X.W. (Xiangchuan Wang); formal analysis, Y.W.; investigation, X.W. (Xinzhong Wang); resources, Y.F.; data curation, C.L.; writing—original draft preparation, J.S.; writing—review and editing, X.W. (Xinzhong Wang); visualization, Y.W.; supervision, J.S.; project administration, C.L.; funding acquisition, X.W. (Xiangchuan Wang). All authors have read and agreed to the published version of the manuscript.

**Funding:** This work was supported by the National Natural Science Foundation of China (Grant No. 51908094) and the Project of the Education Bureau of Hunan Province of China (Grant No. 23B0732, No. 23A0559, and No. 22A0561).

**Data Availability Statement:** The data presented in this study are available from the first and corresponding author upon request. The data are not publicly available due to the policy of the data provider.

**Conflicts of Interest:** Author Xiangchuan Wang was employed by the company Huasheng Testing Technology Co., Ltd. The remaining authors declare that the research was conducted in the absence of any commercial or financial relationships that could be construed as a potential conflict of interest.

## References

1. Liu, J.; Li, X.; Liu, H.; Chen, B. Recent Application and Development of Concrete-Filled Steel Tube Arch Bridges in China. In *Advances in Civil Engineering Materials, Proceedings of the 6th International Conference on Architecture and Civil Engineering (ICACE 2022), Kuala Lumpur, Malaysia, 18 August 2022*; Nia, E.M., Ling, L., Awang, M., Emamian, S.S., Eds.; Springer: Singapore, 2023; pp. 263–272.
2. Zheng, J.; Wang, J.; Mou, T.; Feng, Z.; Han, Y.; Qin, D. Feasibility Study on Design and Construction of Concrete Filled Steel Tubular Arch Bridge with a Span of 700 m. *Chin. Acad. Eng.* **2014**, *16*, 33–37.
3. Tong, K.; Zhang, H.; Zhao, R.; Zhou, J.; Ying, H. Investigation of SMFL Monitoring Technique for Evaluating the Load-Bearing Capacity of RC Bridges. *Eng. Struct.* **2023**, *293*, 116667. [[CrossRef](#)]
4. Yu, M.; Deng, N.; Chen, Q.; Hao, T. Refined Finite Element Analysis of Crack Causes in SRC Arch Rib Bridges Considering Multiple Factors. *Adv. Civ. Eng.* **2018**, *2018*, 2690951. [[CrossRef](#)]

5. Yang, Y.; Luo, X.; Tang, Y.; Wwei, J.; Chen, B. Research on the Ultimate Bearing Capacity and Simplified Design Formulae of Steel Truss Web-Steel Reinforced Concrete (SRC) Composite Arches. *Eng. Mech.* **2017**, *34*, 200–206.
6. Pouraminian, M.; Ghaemian, M. Shape Optimisation of Concrete Open Spandrel Arch Bridges. *Gradjevinar* **2015**, *67*, 1177–1185.
7. Xie, X.; Fu, Y.; Deng, N. Design of Half-Through Cable-Arch Bridge with 700 m Main Span. *J. Southwest Jiaotong Univ.* **2019**, *54*, 1162–1176. [[CrossRef](#)]
8. Huang, Q.; Wei, J.; Chen, B.; Wu, M. Trial-Design Research on 420m SRC-Steel Web Composite Box Arch Bridge. *J. Fuzhou Univ. Nat. Sci. Ed.* **2011**, *39*, 936–940.
9. Huang, Q.; Fu, Y.; Xu, C.; Chen, B. Trial Design Research on Super Long Span Reactive Powder Concrete Arch Bridge. *J. Nanchang Univ. Eng. Technol.* **2015**, *37*, 252–256+266. [[CrossRef](#)]
10. Shao, X.; He, G. Conceptual Design and Feasibility Study of an 800 m Scale Steel-UHPC Composite Truss Arch Bridge. *China J. Highw. Transp.* **2020**, *33*, 73.
11. Zhang, X.; Deng, Z.; Fang, G.; Ge, Y. Theoretical Analysis of Ultimate Main Span Length for Arch Bridge. *Sustainability* **2022**, *14*, 17043. [[CrossRef](#)]
12. Shao, X.; He, G.; Shen, X.; Zhu, P.; Chen, Y. Conceptual Design of 1000 m Scale Steel-UHPFRC Composite Truss Arch Bridge. *Eng. Struct.* **2021**, *226*, 111430. [[CrossRef](#)]
13. Zheng, J.; Du, H.; Mu, T.; Liu, J.; Qin, D.; Mei, G.; Tu, B. Innovations in Design, Construction, and Management of Pingnan Third Bridge—The Largest-Span Arch Bridge in the World. *Struct. Eng. Int.* **2022**, *32*, 134–141. [[CrossRef](#)]
14. Wei, J.; Ying, H.; Yang, Y.; Zhang, W.; Yuan, H.; Zhou, J. Seismic Performance of Concrete-Filled Steel Tubular Composite Columns with Ultra High Performance Concrete Plates. *Eng. Struct.* **2023**, *278*, 115500. [[CrossRef](#)]
15. Wang, X.; Li, L.; Xiang, Y.; Wu, Y.; Wei, M. The Influence of Basalt Fiber on the Mechanical Performance of Concrete-Filled Steel Tube Short Columns under Axial Compression. *Front. Mater.* **2024**, *10*, 1332269. [[CrossRef](#)]
16. Zhang, X.; Zhou, G.; Liu, X.; Fan, Y.; Meng, E.; Yang, J.; Huang, Y. Experimental and Numerical Analysis of Seismic Behaviour for Recycled Aggregate Concrete Filled Circular Steel Tube Frames. *Comput. Concr.* **2023**, *31*, 537.
17. Zhang, X.; Liu, X.; Zhang, S.; Wang, J.; Fu, L.; Yang, J.; Huang, Y. Analysis on Displacement-Based Seismic Design Method of Recycled Aggregate Concrete-Filled Square Steel Tube Frame Structures. *Struct. Concr.* **2023**, *24*, 3461–3475. [[CrossRef](#)]
18. Huang, W.; Lai, Z.; Chen, B.; Xie, Z.; Varma, A.H. Concrete-Filled Steel Tube (CFT) Truss Girders: Experimental Tests, Analysis, and Design. *Eng. Struct.* **2018**, *156*, 118–129. [[CrossRef](#)]
19. Lai, X.; Chen, B.; Zheng, J.; Huang, L. Experimental Study on Stability Capacity of CFT Columns Considering the Influence of Long-Term Load. *Build. Sci.* **2023**, *39*, 65–73.
20. Xu, L.; Lu, Q.; Chi, Y.; Yang, Y.; Yu, M.; Yan, Y. Axial Compressive Performance of UHPC Filled Steel Tube Stub Columns Containing Steel-Polypropylene Hybrid Fiber. *Constr. Build. Mater.* **2019**, *204*, 754–767. [[CrossRef](#)]
21. Shi, Z.; Hu, H.; Li, J. Axis Optimisation of Arch-Shaped Pylons for High-Speed Railway Cable-Stayed Bridges. *Eng. Struct.* **2021**, *227*, 111424. [[CrossRef](#)]
22. Zheng, J.; Wang, J. Concrete-Filled Steel Tube Arch Bridges in China. *Engineering* **2018**, *4*, 143–155. [[CrossRef](#)]
23. Lan, H. Investigation and Analysis of Development Situation of CFST Truss Arch Bridge in China. *West. China Commun. Technol.* **2018**, *7*, 134–138. (In Chinese) [[CrossRef](#)]
24. Chen, B.-W.; Han, L.-H.; Qin, D.-Y.; Li, W. Life-Cycle Based Structural Performance of Long-Span CFST Hybrid Arch Bridge: A Study on Arch of Pingnan Third Bridge. *J. Constr. Steel Res.* **2023**, *207*, 107939. [[CrossRef](#)]
25. Chen, B.; Liu, J.; Habib, T. Recent Research and Application of Arch Bridges in China. In *Proceedings of ARCH 2019, Proceedings of the 9th International Conference on Arch Bridges, Porto, Portugal, 2–4 October 2019*; Arède, A., Costa, C., Eds.; Springer International Publishing: Cham, Switzerland, 2020; pp. 536–544.
26. Fan, Y.; Xin, J.; Yang, L.; Zhou, J.; Luo, C.; Zhou, Y.; Zhang, H. Optimization Method for the Length of the Outsourcing Concrete Working Plane on the Main Arch Rib of a Rigid-Frame Arch Bridge Based on the NSGA-II Algorithm. *Structures* **2024**, *59*, 105767. [[CrossRef](#)]
27. Fan, Y.; Zhou, J.; Luo, C.; Yang, J.; Xin, J.; Wang, S. Research on Loading Scheme for Large-Scale Model Tests of Super-Long-Span Arch Bridge. *Buildings* **2023**, *13*, 1639. [[CrossRef](#)]
28. Chen, B.; Liu, F.; Wei, J. Statistical Analysis of 327 Steel-Tube Concrete Arch Bridges. *J. China Foreign Highw.* **2011**, *31*, 96–103. (In Chinese) [[CrossRef](#)]
29. Ye, W.; Wang, L.; Sun, X.; Xu, D.; Wang, T. Key Parameter Influence Analysis of Half-through Concrete-Filled Steel Tubular Arch Bridge. *Bridge Constr.* **2023**, *53*, 79–86. (In Chinese) [[CrossRef](#)]
30. Chen, B.; Liu, J.; Wei, J. *Concrete-Filled Steel Tubular Arch Bridges*; Springer: Singapore, 2023.
31. Khuri, A.I.; Mukhopadhyay, S. Response Surface Methodology. *Wiley Interdiscip. Rev. Comput. Stat.* **2010**, *2*, 128–149. [[CrossRef](#)]
32. Ye, D.; Xu, Z.; Liu, Y. Solution to the Problem of Bridge Structure Damage Identification by a Response Surface Method and an Imperialist Competitive Algorithm. *Sci. Rep.* **2022**, *12*, 16495. [[CrossRef](#)] [[PubMed](#)]
33. Tang, Q.; Xin, J.; Jiang, Y.; Zhang, H.; Zhou, J. Dynamic Response Recovery of Damaged Structures Using Residual Learning Enhanced Fully Convolutional Network. *Int. J. Struct. Stab. Dyn.* **2024**. [[CrossRef](#)]

- 
34. Temür, R. Analyses of Plane Stress and Plane Strain through Energy Minimization. *Structures* **2021**, *33*, 728–736. [[CrossRef](#)]
  35. Juvinall, R.C.; Marshek, K.M. *Fundamentals of Machine Component Design*; John Wiley & Sons: Hoboken, NJ, USA, 2020.

**Disclaimer/Publisher’s Note:** The statements, opinions and data contained in all publications are solely those of the individual author(s) and contributor(s) and not of MDPI and/or the editor(s). MDPI and/or the editor(s) disclaim responsibility for any injury to people or property resulting from any ideas, methods, instructions or products referred to in the content.